Physica Scripta. Vol. T120, 40–46, 2005

Highly Charged Ion Research at the Livermore Electron Beam Ion Traps

Peter Beiersdorfer[1,*]

[1]High Temperature and Astrophysics Division, University of California, Lawrence Livermore National Laboratory, 7000 East Avenue L-260, Livermore, CA 94550, USA

Received December 26, 2003; accepted January 25, 2004

PACS numbers: 32.30.Jc, 32.30.Rj, 32.80.Fn, 32.60.+i, 32.70.Cs, 32.70.Fw, 34.70.+e, 34.80.−i

Abstract

Spectroscopy performed with the three Livermore electron beam ion traps is reviewed, which is continuing and complementing the innumerable contributions to atomic physics provided over the years by heavy-ion accelerators. Numerous spectrometers were developed that cover the spectral bands from the visible to the hard X-ray region. These enabled exhaustive line surveys useful for X-ray astrophysics and for systematic studies along iso-electronic sequences, such as the 4s-4p, 3s-3p, and 2s-2p transitions in ions of the Cu-I, Na-I, and Li-I sequences useful for studying QED and correlation effects as well as for precise determinations of atomic-nuclear interactions. They also enabled measurements of radiative transition probabilities of very long-lived (milli- and microseconds) and very short-live (femtosecond) levels. Because line excitation processes can be controlled by choice of the electron beam energy, the observed line intensities are used to infer cross sections for electron-impact excitation, dielectronic recombination, resonance excitation, and innershell ionization. These capabilities have recently been expanded to simulate X-ray emission from comets by charge exchange. Specific contributions to basic atomic physics, nuclear physics, and high-temperature diagnostics are illustrated.

1. Introduction

Atomic spectroscopy provides insight into fundamental physics issues. It has been the key for understanding quantum mechanics and quantum electrodynamics. Highly charged ions extend such fundamental studies to the strong electric and nuclear fields produced by heavy nuclei where new phenomena become observable. For example, relativity allows "forbidden" transitions to be prominent; vacuum polarization causes a substantial shift in some energy levels; atomic-nuclear interactions, including the finite size of the nuclear charge and nuclear magnetization distribution, play a significant role; the magnetic interaction, which is negligible at low Z, dominates many electron scattering cross sections for $Z \approx 100$; even tests of the Standard Model are possible, as parity violation may be observable in specific highly charged ionic systems. Highly charged ions are also key for developing diagnostics of high temperature plasmas in magnetic fusion and inertial confinement fusion. Fields such as X-ray astronomy rely almost exclusively on the spectroscopy of highly charged ions, as radiation from ions embedded in hot plasma are the only way to extract information from afar.

Highly charged ions require much more energy to produce and to excite than neutral or near-neutral atoms. A few heavy-ion accelerators have had the energy needed to generate any charge state of any element. The beam-foil technique, in which the fast moving ions from a heavy-ion accelerator interact with the stationary electron cloud in a foil target, represents a good and productive environment for studying the properties of highly charged ions.

*Email address: beiersdorfer@llnl.gov

The electron beam ion trap functions similarly as the heavy ion based beam-foil technique. The difference is that the ions are stationary (apart from thermal motion and oscillatory motion within the trap), and the electrons are moving. In other words, the electron beam ion trap functions with the role of ions and electrons reversed. The advantage is that less energy is consumed to accelerate an electron than an ion to achieve the same collision parameters. For example, an electron accelerated to 200 keV in an ion trap can produce fully stripped uranium [1]. Production of bare uranium in a heavy-ion accelerator requires ions with energy of roughly a hundred GeV [2]. This means that an electron beam ion trap is a considerably smaller device than a heavy-ion accelerator. The electron density in an electron beam ion trap is markedly lower than in that in a solid foil, 10^{11}–10^{12} cm^{-3} versus about 10^{23} cm^{-3}. This means that ionization times, i.e., the time to reach a certain charge state is significantly longer in an electron beam ion trap, typically a few to a few tens of milliseconds, than in the beam-foil interaction, where a given charge state must be reached in the short transit time through a micrometer-thick foil, i.e., a few picoseconds. The longer time scales are no problem as the ion storage time in an electron beam ion trap is typically of the order of seconds to hours [3].

A comparison between electron beam ion traps and the beam-foil technique shows that the two approaches not only can access similar physical states of matter but are complementary to each other. For example, the high electron density in the beam-foil technique allows excitation of levels that are multiply excited, such as sextet levels that cannot or can only be marginally accessed with other techniques [4, 5, 6]. By contrast, the low electron density in the electron beam ion trap allows measurements of slow, electric dipole forbidden transitions, i.e., to record spectral emission in the so-called coronal approximation [7]. Similarly, the beam-foil method allows measurements of the radiative rates of fast dipole-allowed transitions [8], while the electron beam ion trap approach allows to determine the radiative lifetime of long-lived metastable levels [9].

Many years of research on highly charged ions in electron beam ion traps have now been pursued, complementing an even longer period of research with heavy-ion accelerators. Nevertheless, the field of highly charged ion research is still not "exhausted". It is important to note on this occassion when we reflect on many years of accomplishments by Professor Indrek Martinson that the field is as vibrant as ever and much new fundamental and applied research is in the offing. Spectroscopy of highly charged ions, in particular, is a great research area for graduate students and a promising area for starting a career in physics which overlaps many other subfields in physics. Applications in astrophysics and fusion energy research are more abundant than ever, and fundamental

physics studies are becoming more exciting as the achievable precision has increased dramatically over the past years allowing experimental physics to probe atomic processes in unprecedented depth. The increase in precision was achieved with the advent of novel instrumentation based in part on electronic cameras, microcalorimeters, and advanced focusing spectrometers.

In the following we present an overview of highly charged ion research using the electron beam ion traps at the University of California Lawrence Livermore National Laboratory. Applications of this research to astrophysics was reviewed recently [7]. As a result, we will focus instead on presenting an overview of recent fundamental atomic science issues studied with these devices and mention applications to astrophysics only in passing.

2. The Livermore electron beam ion traps and associated instrumentation

The first electron beam ion trap was put into operation in 1986 at the University of California Lawrence Livermore National Laboratory (LLNL). It represented a modified electron beam ion source similar to the devices described by Donets [10, 11]. The device, dubbed EBIT, was quickly followed by a second electron beam ion trap at LLNL, named EBIT-II. Routine operation of EBIT-II commenced in January 1990. Both EBIT and EBIT-II operated at electron beam energies below 40 keV. To address the need for higher electron beam energies EBIT was converted into a new, high-energy electron beam ion trap. This high-voltage machine was named SuperEBIT and commenced routine operation at LLNL in January 1992. SuperEBIT achieved electron beam energies in excess of 200 keV and produced the highest charged ion – Cf^{96+} [12] – so far observed in an electron beam ion trap.

The success of EBIT, EBIT-II, and SuperEBIT prompted the construction of electron beam ion traps outside Livermore. The first two machines outside Livermore were built at Oxford, England [13]. These used a modified Livermore design of EBIT-II. One of these British-built machines is now located the National Institute of Standards in Gaithersburg, Maryland [14]. A third close copy of EBIT-II was built in the United States and now operates at the Institute for Plasma Physics in Berlin [15]. Additional machines are operating at the University of Electro-Communications, Tokyo, the Max-Planck-Institute in Heidelberg, Germany, and at the Technical University, Dresden, Germany [16, 17, 18].

Because "EBIT" has now been used to denote a variety of electron beam ion traps, we now refer to the orginal EBIT as EBIT-I to avoid confusion. This distinction is necessary because the performance characteristics and operating parameters vary considerably from machine to machine. After an internal move, both EBIT-I and SuperEBIT are now operating at LLNL in alternation depending on the science needs.

Various operating modes have been developed at LLNL. These have continued to enable access to new physics regimes. Complementing the "electron trapping" mode, which is the normal mode of operation of an EBIT, we employ the "magnetic trapping" mode [19, 20, 21], which allows us to study ions confined in a Penning trap in the absence of the electron beam. Another mode is the "thermal plasma" or "Maxwellian" mode. In this mode the electron beam maps out in time a Maxwellian electron energy distribution [22]. We use this mode to study the spectral emission as a function of electron *temperature*. We have also developed the "inverted-trap" mode [23], which provides spectra of neutral and few-charge ions of any element that can be introduced as a volatile substance into the trapping region. These advanced operating modes are paired with an upgraded data acquisition system that provides multiparameter digitization of several dozen parameters simultaneously and allows us to perform detailed measurements of electron-ion interaction cross sections, charge transfer, radiative decay rates, and ionization balance evolution [24].

The development of unique spectral equipment is crucial for advances in highly charged ion physics. In order to take advantage of the opportunities provided by the different operating modes we have developed a variety of spectroscopic instrumentation. This includes high-resolution bent X-ray crystal spectrometers for the 1 to 5 Å range in the von Hámos geometry [25, 26] for which we developed multi-wire proportional counters [27]. We also developed several flat-crystal spectrometers for the 4 to 20 Å range [28, 29, 30]. The EUV and X-ray band is also covered with an advanced high-resolution multi-pixel microcalorimeter [31]. For the hard X-ray range below 1 Å we developed a transmission spectrometer in the Du Mond geometry [32] that complements a variety of high-purity Ge and IGLET detectors. The soft X-ray and extreme ultraviolet wavelength band is accessed with a variety of grazing incidence grating spectrometers [33, 34], while we use a normal incidence spectrometer to measure lines in the far UV and optical regimes [35]. Two high-resolution transmission grating spectrometers were developed for the visible [36], and a filter-based instrument was developed to record the radiative rates of visible transitions [37]. As one can see from this discussion, we have developed instrumentation covering the entire spectral band from the hard X-ray to the visible wavelength regime and spanning five orders of magnitude in photon energy.

3. Atomic-nuclear interactions

The wave function of the 1s electron overlaps with the nucleus more than that of any other electron. The overlap means that the 1s electron represents a sensitive probe of nuclear properties. In fact, the 1s wave function is sensitive to the size and shape of the distribution of nuclear charge. This "finite nuclear size" effect is a major contribution to the Lamb shift [38].

The 1s wave function is also very sensitive to the size and distribution of the nuclear magnetic moment. In atomic hydrogen, the interaction between the magnetic moment of the nucleus and the electron spin of the 1s electron results in the well known 21-cm line. The same interaction can be found in hydrogenlike ions. The 1s hyperfine splitting of heavy highly charged ions is as large as several eV. This means that the photons emitted by heavy hydrogenlike ions are in the optical wavelength band.

We have made measurements of the 1s hyperfine splitting in several hydrogenlike ions, as can be seen from Table I. Most recently we used the high-resolution transmission grating spectrometer [36] to measure the 1s hyperfine transitions of ^{203}Tl and ^{205}Tl [39], which are the most accurate measurements to date.

Given that hydrogenlike ions are the Rosetta Stone of quantum mechnanics, there is a suprisingly large discrepancy between the measured values and theory. For example, the calculated transition wavelengths for ^{205}Tl are 3786 Å [40], 3802 Å [41] and 3849 Å [42]. These vary by about 60 Å amongst each other and differ between -36 and $+27$ Å from the measured value of 3821.84 ± 0.34 Å [39]. The differences may be caused by inaccuracies in various fundamental properties of these ions, including finite charge effects, the value of the nuclear magnetic

Table I. *Overview of all 1s hyperfine transition measurements in heavy hydrogenlike ions. ESR is the heavy-ion storage ring at GSI Darmstadt.*

Ion	Facility	Energy (KeV)	Reference
$^{207}Pb^{81+}$	ESR	1.2159 ± 0.0002	[81]
$^{165}Ho^{66+}$	SuperEBIT	2.1645 ± 0.0006	[82]
$^{185}Re^{74+}$	SuperEBIT	2.7190 ± 0.0018	[83]
$^{187}Re^{74+}$	SuperEBIT	2.7450 ± 0.0018	[83]
$^{209}Bi^{82+}$	ESR	5.0840 ± 0.0008	[84]
$^{203}Tl^{80+}$	SuperEBIT	3.21351 ± 0.00025	[39]
$^{205}Tl^{80+}$	SuperEBIT	3.24409 ± 0.00029	[39]

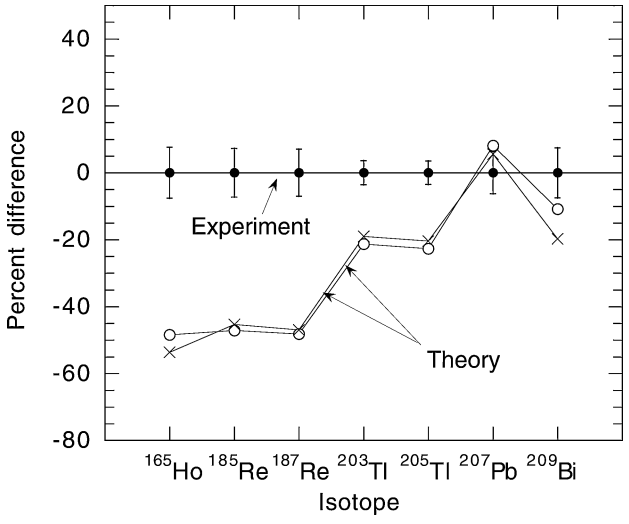

Fig. 1. Percent difference of the calculated and measured Bohr-Weisskopf contributions. All values are referenced to the experimental data shown as solid circles. Theoretical values are from [41] (open circles) and [46] (crosses) who both use the single particle model for calculating the contribution of the nuclear magnetization distribution.

moment, the self energy, and vacuum polarization contributions. At present, it is most likely that the difference is caused by the finite extent of the nuclear magnetization [43].

The results have been used to infer the distribution of the nuclear magnetization [44], i.e., the so-called Bohr-Weisskopf effect. From the values we infer we find that models based on unpaired nucleons to determine the nuclear magnetization cannot accurately describe the observations. This is true in particular for those ions whose nuclear structure is far from a closed shell, as shown in Fig. 1. Unfortunately, calculations based on potentially more sophisticated models [42, 45] produce similar discrepancies, though with less clear or no systematics [44], and thus provide less insight into the underlying physics than the calculations in [41, 46].

In Table I we list the values of the five 1s hyperfine splittings measured on the Livermore SuperEBIT. We also list the two values available from heavy-ion accelerators. One of the accelerator values is in the UV, the other is in the infrared wavelength. All of the SuperEBIT values are in the visible. This table again shows the complementarity between heavy-ion accelerators and electron beam ion trap measurements.

Calculations of the hyperfine structure have been extended to the 2s electron of Li-like ions where they are not only important for fundamental atomic and nuclear physics but also for astrophysics [43, 47, 48]. But only one corresponding measurement, again carried out on SuperEBIT, has so far been made [49]. This field is still wide open and promises exciting results in the future.

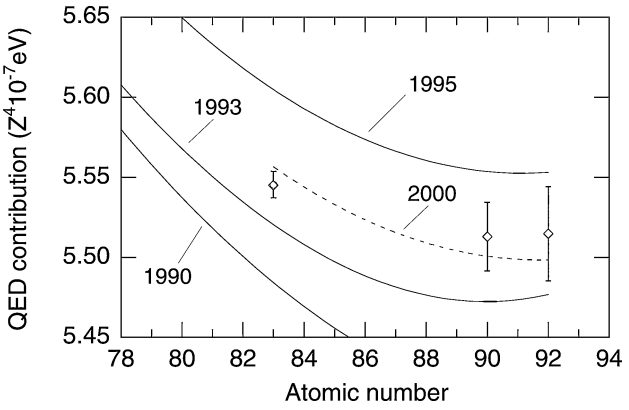

Fig. 2. Comparison of the measured and calculated QED contribution to the $2s_{1/2}$-$2p_{3/2}$ transition in highly charged Li-like ions. The measured values are from Refs. [49, 85, 86]. The theoretical values are from Refs. [87], [88], [89], and [90] and are labeled by the year of publication.

4. Tests of strong-field QED

Quantum electrodynamics (QED) is an extremely successful theory. However, tests of QED in the ultra-strong nuclear fields of heavy ions are still needed. In particular, tests of QED are not complete until experiments provide data with sufficient accuracy to test second order QED predictions (two-loop diagrams) in such ions.

QED affects mainly s electrons. Measurements have, therefore, focused on transitions involving 1s, 2s, 3s, and 4s electrons in hydrogenlike, lithiumlike, sodiumlike, and copperlike ions, respectively.

The accuracy of 1s QED measurements is still too poor to test QED terms to better than a few percent [50]. The accuracy of 2s QED measurements, however, at the Livermore SuperEBIT facility has approached 1.5×10^{-3} (or 9×10^{-4} of the Lamb shift) [50]. This is sufficient to distinguish among different theoretical approaches, as shown in Fig. 2. In fact, it is sufficient to be sensitive to two-loop QED calculations [51]. These measurements involve the $2s_{1/2}$-$2p_{3/2}$ transitions. Measurements of the $2s_{1/2}$-$2p_{1/2}$ transitions are now under way on SuperEBIT [52] that should further improve the achieved accuracy of the 2s QED determinations.

Electron beam ion trap measurements at Livermore have also made progress in understanding calculations involving the 3s electron in Na-like ions. Recent measurements of the $3s_{1/2}$-$3p_{3/2}$ transition in U^{81+} have validated *ab initio* QED calculations at the expense of semi-empirical estimates or calculations that involve scaled QED contributions [53], as shown in Fig. 3. The figure once again shows the complementarity of the Livermore ion trap measurements and beam-foil spectroscopy.

Progress has also been made in measuring the $4s_{1/2}$-$4p_{3/2}$ transitions in Cu-like ions [54]. The high-Z experimental trend established by measurements using laser-produced plasmas have been corrected with measurements on the Livermore EBIT-II electron beam ion trap.

5. Isoelectronic trends of complex ions

The study of isoelectronic trends of complex ions for which few or no spectroscopically reliable predictions exist has been a corner stone of accelerator-based spectroscopy [55, 56, 57]. We are continuing such measurements on the Livermore electron

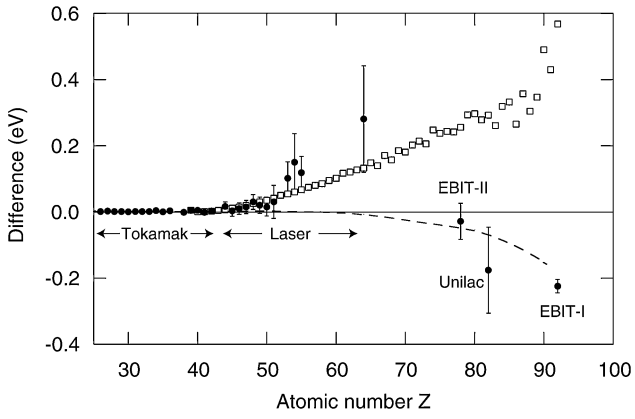

Fig. 3. Comparison of experimental and theoretical $3s_{1/2}$-$3p_{3/2}$ transition energies of sodiumlike ions. All values are referenced to the calculations by Kim *et al*. [91] (solid line). Open squares represent semi-empirical predictions by Seely *et al*. [92]; the dashed line represents the calculations by Blundell [88]. Experimental values from [53, 92, 93, 94, 95, 96] are shown as solid circles and are labeled with the source producing the respective ions.

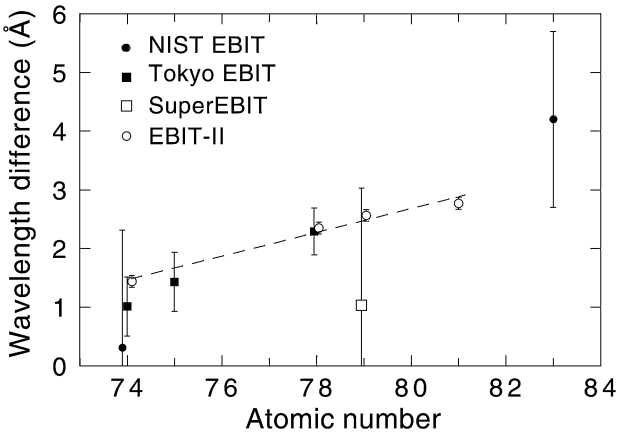

Fig. 4. Comparison of experimental and theoretical wavelength data of the $3s^23p^63d^4$ $J = 2$–3 transition in the high-Z range of Ti-like ions. The measured values are from [97, 61, 98, 99, 62]. All values are referenced to the calculations of Kato *et al*. (solid line) [100]. The dashed line serves to guide the eye and connects the EBIT-II results.

beam ion traps. In addition, we are studying complete spectra in a given wavelength range, such as the L-shell spectra of Si, S, Ar, and Fe in the EUV or X-ray range [58, 59, 60], as discussed by J. K. Lepson in this volume.

A recent example of transitions studied along the isoelectronic sequence is provided by Fig. 4, which shows the $3s^23p^63d^4$ $J = 2$–3 transition in the ground configuration of high-Z Ti-like ions. The values from EBIT-II [61, 62] allow for improved comparison with theory.

In Fig. 5 we show the isoelectronic trend of the transition between the ground state and the $1s^22s2p^2\ ^2P_{3/2}$ level in B-like ions. We have contributed only one datum so far to this plot, namely for xenon. This point was measured on SuperEBIT [52]. The point deviates strongly from the isoelectronic trend set by earlier measurements and theory. This clearly illustrates the necessity of extending such measurements to highly charged ions.

6. Transition probabilities

Measurements of radiative transition probabilities study different aspects of the wave functions describing a given system than transition energy measurements and thus provide information

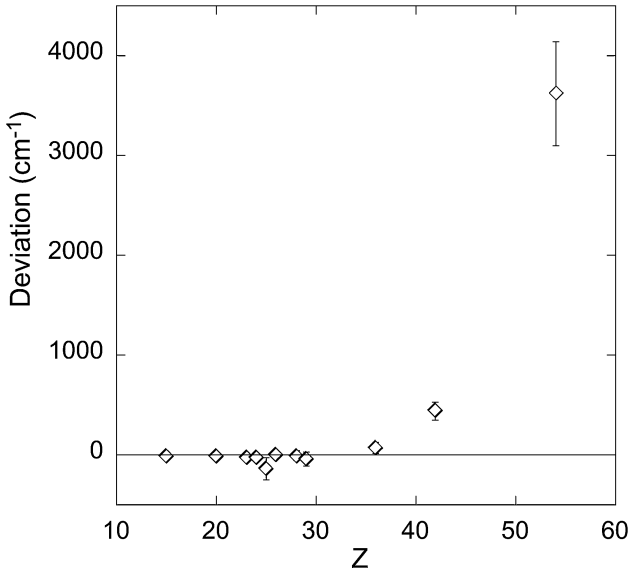

Fig. 5. Comparison of experimental data of the $1s^22s2p^2\ ^2P_{3/2}$ level for mid-Z ions of the B-I isoelectronic sequence relative to the calculations of Safronova *et al.* [101]. For low nuclear charges Z the experimental error bars are smaller than the symbol size.

necessary for improved calculations. They are also important for developing and calibrating a variety of spectral diagnostics.

Measurements of the radiative decay rates of metastable levels using the Livermore electron beam ion traps are discussed by E. Träbert in this volume and in [9]. Many such measurements are made possible by the magnetic mode of operation [21].

Here we point out that very large transition probabilities of X-ray lines corresponding to femtosecond lifetimes can also be measured with the Livermore electron beam ion traps. This is done by observing the natural line width. This technique is similar to what has been done on accelerators for neutral atoms [63] and light ions [64, 65].

The natural line width is related to the radiative lifetime by the uncertainty principle. As a result, such measurements require the very high-resolution X-ray spectrographs we developed at Livermore [66]. They also require that the natural line width is not obscured by other line broadening effects. In the case of ion traps this means that the ion temperature is sufficiently low. Methods to reduce the ion temperature to below a few eV/amu have been discussed and successfully applied [67, 68]. The technique resulted in the first measurements of the radiative lifetime of a highly charged ion in the femtosecond regime [69, 70]. Figure 6 shows the measured line shape of the $(2p^6)_{J=0}$-$(2p^5_{3/2}3d_{5/2})_{J=1}$ transition in neonlike Cs^{45+} and its associated Lorentzian fit. The radiative lifetime of its upper level inferred from these and other data is 1.65 fs.

Systematic measurements of femtosecond radiative lifetimes are just beginning and are needed in a variety of situations. Fast transition rates correspond to large absorption oscillator strengths. As a result, the radiative rates of dipole-allowed transitions in highly charged ions dominate the Planck mean opacity of a high-temperatures plasma. Accurate knowledge of these rates is, therefore, important for plasma opacity and line transfer determinations.

7. Magnetic field sensitive lines

Developing and calibrating spectral lines for plasma diagnostics is one of the most important tasks of atomic spectroscopy.

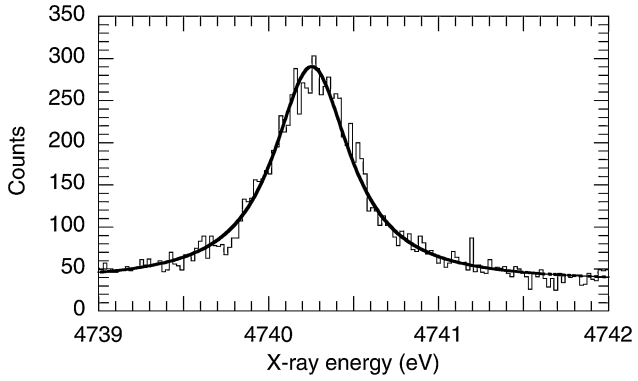

Fig. 6. Observed lineshape of the $2p_{3/2}$-$3d_{5/2}$ transition in Cs^{45+} at an ion temperature of 110 eV. The goodness of a least-squares fit with a Lorentzian trial function (thick solid line) indicates that the line shape is dominated by the natural line width.

X-ray lines are used, for example, for measurements of plasma temperature, density, bulk motion, ionization balance, and elemental abundances. The magnetic field strength is another fundamental plasma parameter. However, no X-ray line diagnostics of magnetic field strength existed until very recently.

The first magnetic field X-ray line diagnostics was developed using the Livermore electron beam ion trap. We showed that magnetic fields can induce X-ray decay of certain levels that are normally strictly forbidden from doing so [71]. In particular, we found that the $(2p^5_{1/2}3s)_{J=0}$ level in neonlike ions can decay to the $2p^6_{J=0}$ neonlike ground state in the presence of a sufficiently strong magnetic field. The $(2p^5_{1/2}3s)_{J=0}$ level mixes with the neighboring $(2p^5_{1/2}3s)_{J=1}$ level, making decay to the ground state possible [71]. The decay rate resulting from this mixing is proportional to the square of the magnetic field strength. For Ar^{8+} ions embedded in a 3 T field the rate is about half the size of the radiative decay rate of the $(2p^5_{3/2}3s)_{J=2}$ level that produces the well known magnetic quadrupole line (cf. Fig. 7). It by far exceeds the competing M1 decay rate of the $(2p^5_{1/2}3s)_{J=0} \rightarrow (2p^5_{3/2}3s)_{J=1}$ transition.

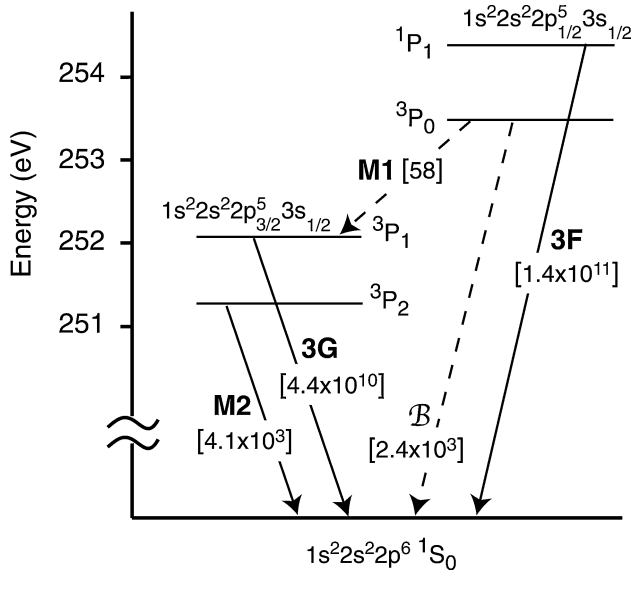

Fig. 7. Grotrian diagram showing the lowest four excited levels in Ar^{8+}. Calculated radiative transition rates (in units of s^{-1}) are indicated in square brackets assuming a 3-T magnetic field. At this field strength the M1 rate induced by the magnetic field is more than half of that of the M2 rate.

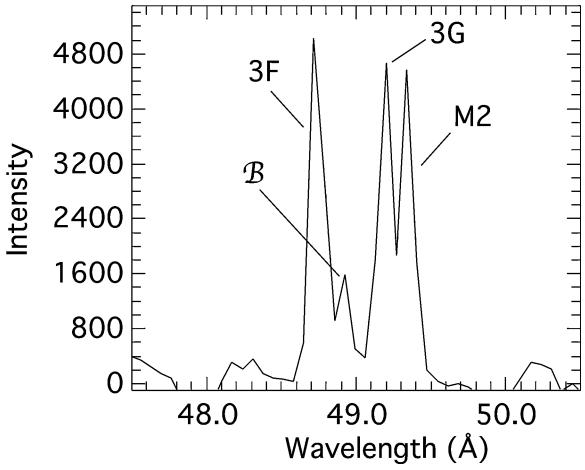

Fig. 8. Spectrum of the Ar^{8+} 2p-3s emission at an electron density of $n \approx 1.25 \times 10^{10}\,cm^{-3}$ measured on EBIT-I. The lines are labeled using the notation defined in Fig. 7.

The magnetic field sensitive line, labeled $\mathcal{B}$, resulting from the decay of the $(2p^5_{1/2}3s)_{J=0}$ level is readily observed in the L-shell spectrum of Ar^{8+}, as seen in Fig. 8. The principle behind this line diagnostic applies to all neonlike ions, and thus different magnetic fields can be measured with different neonlike ions. Moreover, the principle also applies to other ions where mixing between an otherwise weak or forbidden line with a strong dipole-allowed transition is possible. More research into magnetic field sensitive lines will be necessary to identify and calibrate all the diagnostically useful cases.

8. Charge exchange measurements with a multi-pixel microcalorimeter

Charge-exchange measurements are also complementary to accelerator-based experiments. Instead of a fast ion beam interacting with neutral target atoms, neutral gases are injected into the ion trap and made to interact with the ions at low collision energies. The collision energy in the electron beam ion trap is determined by the ion temperature, which, as indicated in Section 6, can be varied and can reach rather low values (below 1 eV/amu [69]).

Charge-exchange measurements using the Livermore electron beam ion traps utilize the magnetic trapping mode [21, 72]. The reactions are studied by recording the X-rays given off during the recombination process. The technique has been applied to ions with charge as high as U^{91+} [73, 74].

Most recently the technique has been applied to simulate the X-ray emission from comets interacting with the solar wind [75]. For this simulation a complete survey of the K-shell X-ray emission of C, N, O, and Ne was needed. This was accomplished using time-resolved X-ray spectroscopy, and the resulting experimental data were successfully used to fit the spectrum of comet Linear observed with the Chandra X-ray Observatory [75].

A typical spectrum of the X-ray emission of O^{7+} following charge exchange between O^{8+} and CH_4 is shown in Fig. 9. A signature of charge exchange is strong emission from levels with high principal quantum number. The spectrum in Fig. 9, for example, shows enhanced emission from $n = 5$ and 6. In other words, the Lyman-δ and Lyman-ϵ lines are stronger that the Lyman-γ line.

These measurements utilized a 6 × 6-pixel microcalorimeter array built at the Goddard Space Flight Center [31].

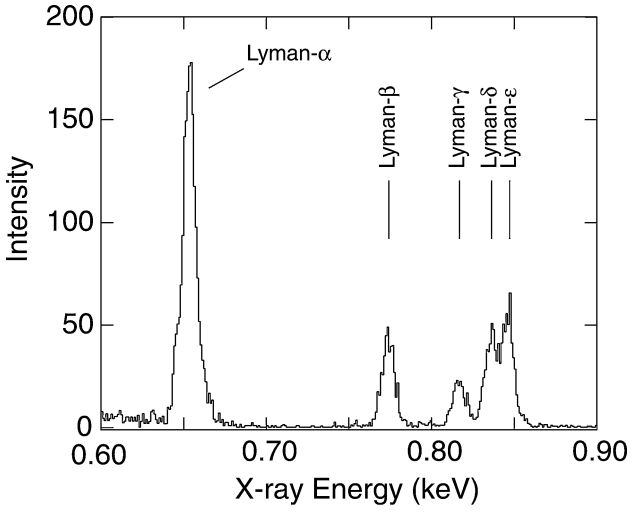

Fig. 9. K-shell emission spectrum of O^{7+} produced by charge exchange between neutral CH_4 and O^{8+} ions. The measurements were made with the Goddard 6×6 multi-pixel microcalorimeter on EBIT-I.

Microcalorimeters have been a mainstay of measurements on the Livermore electron beam ion traps. The multi-pixel, 10-eV resolution Goddard instrument on EBIT-I followed a single-pixel calorimeter with 25-eV energy resolution and a 0.25 mm^2 detection area first used for *in situ* measurements on EBIT-II in 1995 [76]. The single-pixel instrument was briefly implemented with improved energy resolution at the NIST electron beam ion trap [77]. A large area detector, as provided by the 6×6 pixel array, however, was necessary to record the weak signal level produced by charge exchange reactions during the magnetic trapping mode.

The multi-pixel microcalorimeter has been used since 2000 in situations where broadband spectral coverage is needed. Charge exhange is one very important research area. Others concern measurements of absolute excitation cross sections [78] and the calibration of relative intensity ratios [79].

9. Conclusion

Much of the research reviewed here was stimulated early on by the examples set by Professor Martinson in his beam-foil measurements at Lund [80]. Our summary of highly charged ion research at the University of California Lawrence Livermore National Laboratory shows that atomic spectroscopy continues to provide a rich area of research interconnected with many important subfields of physics including nuclear physics, X-ray astronomy, plasma physics, and basic atomic physics. The fact that much remains to be done and unforeseen areas keep adding new opportunities means that graduate students will find a nourishing environment for years to come. On the occasion of Professor Martinson's retirement we can note that the field has expanded well beyond the beginnings of beam-foil spectroscopy, and we look forward to many new discoveries in the future.

Acknowledgements

This work was supported in part by NASA's Space Astrophysics Research and Analysis program and performed under the auspices of the US Department of Energy by the University of California Lawrence Livermore Natonal Laboratory under Contract W-7405-Eng-48.

References

1. Marrs, R. E., Elliott, S. R. and Knapp, D. A., Phys. Rev. Lett. **72**, 4082 (1994).
2. Kienle, P., Physica Scripta **T46**, 81 (1993).
3. Schneider, M. B. *et al*., in International Symposium on Electron Beam Ion Sources and their Applications – Upton, NY 1988, AIP Conference Proceedings No. 188, (edited by A. Hershcovitch), (AIP, New York, 1989), p. 158.
4. Blanke, J. H., Fricke, B., Heckmann, P. H. and Träbert, E., Physica Scripta **45**, 430 (1992).
5. Träbert, E., Fritsche, S. and Jupén, C., Eur. Phys. J. D **3**, 13 (1998).
6. Lapierre, A. and Knystautas, E. J., J. Phys. B **33**, 2245 (2000).
7. Beiersdorfer, P., Ann. Rev. Astron. Astrophys. **412**, 343 (2003).
8. Curtis, L. J. and Martinson, I., Comm. At. Mol. Phys. **24**, 213 (1990).
9. Träbert, E., Can. J. Phys. **80**, 1481 (2002).
10. Donets, E. D., Physica Scripta **T3**, 11 (1983).
11. Levine, M. A. *et al*., Nucl. Instrum. Meth. **B43**, 431 (1989).
12. Beiersdorfer, P., Elliott, S. R., Crespo López-Urrutia, J. and Widmann, K., Nucl. Phys. **A626**, 357 (1997).
13. Silver, J. D. *et al*., Rev. Sci. Instrum. **65**, 1072 (1994).
14. Gillaspy, J. D. *et al*., Physica Scripta **T59**, 392 (1995).
15. Biedermann, C., Förster, A., Fußmann, G. and Radtke, R., Physica Scripta **T73**, 360 (1997).
16. Nakamura, N. *et al*., Rev. Sci. Instrum. **69**, 694 (1998).
17. Ovsyannikov, V. P. and Zschornack, G., Rev. Sci. Instrum. **70**, 2646 (1999).
18. Crespo López-Urrutia, J. R., Bapat, B., Draganic, I., Werdich, A. and Ullrich, J., Physica Scripta **T92**, 110 (2001).
19. Beiersdorfer, P., Beck, B., Marrs, R. E., Elliott, S. R. and Schweikhard, L., Rapid Commun. Mass Spectrom. **8**, 141 (1994).
20. Beiersdorfer, P., Beck, B., Becker, S. and Schweikhard, L., Int. J. Mass Spectrom. Ion Proc. **157/158**, 149 (1996).
21. Beiersdorfer, P., Schweikhard, L., Crespo López-Urrutia, J. and Widmann, K., Rev. Sci. Instrum. **67**, 3818 (1996).
22. Savin, D. W. *et al*., Rev. Sci. Instrum. **71**, 3362 (2000).
23. Chen, H. *et al*., Physica Scripta **T92**, 284 (2001).
24. Beiersdorfer, P., Brown, G. V., Hildebrandt, L., Wong, K. L. and Ali, R., Rev. Sci. Instrum. **72**, 508 (2001).
25. Beiersdorfer, P. *et al*., Rev. Sci. Instrum. **61**, 2338 (1990).
26. Beiersdorfer, P., Nucl. Instrum. Meth. **B56/57**, 1144 (1991).
27. Vogel, D., Beiersdorfer, P., Decaux, V. and Widmann, K., Rev. Sci. Instrum. **66**, 776 (1995).
28. Beiersdorfer, P. and Wargelin, B. J., Rev. Sci. Instrum. **65**, 13 (1994).
29. Beiersdorfer, P., Crespo-López Urrutia, J. R., Förster, E., Mahiri, J. and Widmann, K., Rev. Sci. Instrum. **68**, 1077 (1997).
30. Brown, G. V., Beiersdorfer, P. and Widmann, K., Rev. Sci. Instrum. **70**, 280 (1999).
31. Porter, F. S. *et al*., Proc. SPIE **4140**, 407 (2000).
32. Widmann, K. *et al*., Rev. Sci. Instrum. **68**, 1087 (1997).
33. Beiersdorfer, P., Crespo López-Urrutia, J. R., Springer, P., Utter, S. B. and Wong, K. L., Rev. Sci. Instrum. **70**, 276 (1999).
34. Utter, S. B., Brown, G. V., Beiersdorfer, P., Clothiaux, E. J. and Podder, N. K., Rev. Sci. Instrum. **70**, 284 (1999).
35. Utter, S. B., Beiersdorfer, P., Crespo López-Urrutia, J. R. and Träbert, E., Rev. Sci. Instrum. **70**, 288 (1999).
36. Utter, S. B., López-Urrutia, J. R. C., Beiersdorfer, P. and Träbert, E., Rev. Sci. Instrum. **73**, 3737 (2002).
37. Träbert, E. and Beiersdorfer, P., Rev. Sci. Instrum. **74**, 2127 (2003).
38. Johnson, W. R. and Soff, G., At. Data Nucl. Data Tables **33**, 405 (1985).
39. Beiersdorfer, P. *et al*., Phys. Rev. A **64**, 032506 (2001).
40. Shabaev, V. M., J. Phys. B **27**, 5825 (1994).
41. Gustavsson, M. G. H., Forssén, C. and Mårtensson-Pendrill, A.-M., Hyperf. Int. **127**, 347 (2000).
42. Tomaselli, M. *et al*., Phys. Rev. A **65**, 022502 (2002).
43. Shabaev, V. M., Artemyev, A. N., Yerokhin, V. A., Zherebtsov, O. M. and Soff, G., Phys. Rev. Lett. **86**, 3959 (2001).
44. Beiersdorfer, P. *et al*., Nucl. Instrum. Meth. **B 205**, 63 (2003).
45. Boucard, S. and Indelicato, P., Eur. Phys. J. D **8**, 59 (2000).
46. Shabaev, V. M., Tomaselli, M., Kühl, T., Artemyev, A. N. and Yerokhin, V. A., Phys. Rev. A **56**, 252 (1997).
47. Shabaev, V. M., Shabaeva, M. B. and Tupitsyn, I. I., Phys. Rev. A **52**, 3686 (1995).
48. Sapirstein, J. and Cheng, K. T., Phys. Rev. A **63**, 032506 (2001).

49. Beiersdorfer, P., Osterheld, A., Scofield, J., Crespo López-Urrutia, J. and Widmann, K., Phys. Rev. Lett. **80**, 3022 (1998).
50. Beiersdorfer, P., Widmann, K. and Crespo López-Urrutia, J. R., Hyperfine Interactions **114**, 141 (1998).
51. Sapirstein, J. and Cheng, K. T., Phys. Rev. A **64**, 022502 (2001).
52. Träbert, E., Beiersdorfer, P., Lepson, J. K. and Chen, H., Phys. Rev. A **68**, 042501 (2003).
53. Beiersdorfer, P. *et al*., Phys. Rev. A **67**, 052103 (2003).
54. Utter, S. B., Beiersdorfer, P., Träbert, E. and Clothiaux, E. J., Phys. Rev. A **67**, 032502 (2003).
55. Martinson, I., Rep. Prog. Phys. **52**, 157 (1989).
56. Martinson, I., Nucl. Instrum. Meth. **B43**, 323 (1989).
57. Martinson, I. and Curtis, L., Contemp. Phys. **30**, 173 (1989).
58. Brown, G. V. *et al*., Astrophys. J. Suppl. **140**, 589 (2002).
59. Lepson, J. K. *et al*., Astrophys. J. **578**, 648 (2002).
60. Lepson, J. K., Beiersdorfer, P., Behar, E. and Kahn, S. M., Astrophys. J. **590**, 604 (2003).
61. Utter, S. B., Beiersdorfer, P. and Brown, G. V., Phys. Rev. A **61**, 030503 (2000).
62. Utter, S. B., Beiersdorfer, P. and Träbert, E., Phys. Rev. A **67**, 012508 (2003).
63. Berry, H. G., Desesquelles, J. and Duffay, M., Phys. Lett. **36A**, 237 (1971).
64. Mannervik, S., Cederquist, H. and Kisielinski, M., Physica Scripta **T8**, 107 (1984).
65. Mannervik, S., Physica Scripta **40**, 28 (1989).
66. Beiersdorfer, P., in AIP Conference Proceedings 389, X-Ray and Innershell Processes, AIP, (edited by R. L. Johnson, H. Schmidt-Böcking and B. F. Sonntag), (AIP, Woodbury, NY, 1997), p. 121.
67. Beiersdorfer, P., Decaux, V., Elliott, S., Widmann, K. and Wong, K., Rev. Sci. Instrum. **66**, 303 (1995).
68. Beiersdorfer, P., Decaux, V. and Widmann, K., Nucl. Instrum. Meth. **B98**, 566 (1995).
69. Beiersdorfer, P., Osterheld, A. L., Decaux, V. and Widmann, K., Phys. Rev. Lett. **77**, 5353 (1996).
70. Graf, A., Beiersdorfer, P., Harris, C. L., Hwang, D. Q. and Neill, P. A., in "Spectral Line Shapes", CP645 (ed. by C. A. Back), (AIP, New York, 2002), p. 74.
71. Beiersdorfer, P., Scofield, J. H. and Osterheld, A. L., Phys. Rev. Lett. **90**, 235003 (2002).
72. Beiersdorfer, P. *et al*., Physica Scripta **T80**, 121 (1999).
73. Schweikhard, L. *et al*., Nucl. Instrum. Meth. **B 142**, 245 (1998).
74. Beiersdorfer, P. *et al*., Phys. Rev. Lett. **85**, 5090 (2000).
75. Beiersdorfer, P. *et al*., Science **300**, 1461 (2003).
76. Gros, M. L. *et al*., in "Electron Beam Ion Trap Annual Report 1995", University of California Lawrence Livermore National Laboratory Report UCRL-ID-124429 (Livermore, 1996), p. 22 (1995).
77. Silver, E. *et al*., Astrophys. J. **541**, 495 (2000).
78. Chen, H. *et al*., Astrophys. J. (Lett.) **567**, L169 (2002).
79. Beiersdorfer, P. *et al*., Astrophys. J. (Lett.) **576**, L169 (2002).
80. Martinson, I., in 33rd Scottish Universities Summer School in Physics, Astrophysical Plasma Spectroscopy, St. Andrews (edited by J. Lang, *et al*.), (SUSSP Publications, University of Edingburgh, Edinburgh, 1988), p. 339–365.
81. Seelig, P. *et al*., Phys. Rev. Lett. **81**, 4824 (1998).
82. López-Urrutia, J. R. C., Beiersdorfer, P., Savin, D. W. and Widmann, K., Phys. Rev. Lett. **77**, 826 (1996).
83. López-Urrutia, J. R. C. *et al*., Phys. Rev. A **57**, 879 (1998).
84. Klaft, I. *et al*., Phys. Rev. Lett. **73**, 2425 (1994).
85. Beiersdorfer, P., Knapp, D., Marrs, R. E., Elliott, S. R. and Chen, M. H., Phys. Rev. Lett. **71**, 3939 (1993).
86. Beiersdorfer, P. *et al*., Phys. Rev. A **52**, 2693 (1995).
87. Indelicato, P. and Desclaux, J. P., Phys. Rev. A **42**, 5139 (1990).
88. Blundell, S. A., Phys. Rev. A **47**, 1790 (1993).
89. Chen, M. H., Cheng, K. T., Johnson, W. R. and Sapirstein, J., Phys. Rev. A **52**, 266 (1995).
90. Cheng, K. T., Chen, M. H. and Sapirstein, J., Phys. Rev. A **62**, 054501 (2000).
91. Kim, Y.-K., Baik, D. H., Indelicato, P. and Desclaux, J. P., Phys. Rev. A **44**, 148 (1991).
92. Seely, J. F. *et al*., At. Data Nucl. Data Tables **47**, 1 (1991).
93. Reader, J. *et al*., J. Opt. Soc. Am. B **4**, 1821 (1987).
94. Seely, J. F., Feldman, U., Brown, C. M., Dietrich, D. D. and Behring, W. E., J. Opt. Soc. Am. B **5**, 785 (1988).
95. Cowan, T. E. *et al*., Phys. Rev. Lett. **66**, 1150 (1991).
96. Simionovici, A. *et al*., Phys. Rev. A **48**, 3056 (1993).
97. Träbert, E., Beiersdorfer, P., Utter, S. B. and Crespo López-Urrutia, J., Physica Scripta **58**, 599 (1998).
98. Porto, J. V., Kink, I. and Gillaspy, J. D., Phys. Rev. A **61**, 054501 (2000).
99. Watanabe, H. *et al*., Phys. Rev. A **63**, 042513 (2001).
100. Kato, D. *et al*., in Proceedings of the International Seminar on Atomic Processes in Plasmas, July 29–30, 1999, Toki, Japan, NIFS-PROC-44, (ed. I. Murakami and T. Kato), (National Institute of Fusion Science, Toki, 2000).
101. Safronova, M. S., Johnson, W. R. and Safronova, U. I., Phys. Rev. A **54**, 2850 (1996).